Radar Rainfall Estimation for Ground Validation Studies of the Tropical Rainfall Measuring Mission

GRZEGORZ J. CIACH

Iowa Institute of Hydraulic Research, University of Iowa, Iowa City, Iowa

WITOLD F. KRAJEWSKI

Iowa Institute of Hydraulic Research and Department of Civil Engineering, University of Iowa, Iowa City, Iowa

EMMANOUIL N. ANAGNOSTOU AND MARY L. BAECK

Iowa Institute of Hydraulic Research, University of Iowa, Iowa City, Iowa

JAMES A. SMITH

Department of Civil Engineering and Operations Research, Princeton University, Princeton, New Jersey

JEFFREY R. MCCOLLUM AND ANTON KRUGER

Iowa Institute of Hydraulic Research, University of Iowa, Iowa City, Iowa

(Manuscript received 1 December 1995, in final form 15 November 1996)

ABSTRACT

This study presents a multicomponent rainfall estimation algorithm, based on weather radar and rain gauge network, that can be used as a ground-based reference in the satellite Tropical Rainfall Measuring Mission (TRMM). The essential steps are constructing a radar observable, its nonlinear transformation to rainfall, interpolation to rectangular grid, constructing several timescale accumulations, bias adjustment, and merging of the radar rainfall estimates and rain gauge data. Observations from a C-band radar in Darwin, Australia, and a local network of 54 rain gauges were used to calibrate and test the algorithm. A period of 25 days was selected, and the rain gauges were split into two subsamples to apply cross-validation techniques.

A Z–R relationship with continuous range dependence and a temporal interpolation scheme that accounts for the advection effects is applied. An innovative methodology was used to estimate the algorithm controlling parameters. The model was globally optimized by using an objective function on the level of the final products. This is equivalent to comparing hundreds of Z–R relationships using a uniform and representative performance criterion. The algorithm performance is fairly insensitive to the parameter variations around the optimum. This suggests that the accuracy limit of the radar rainfall estimation based on power-law Z–R relationships has been reached. No improvement was achieved by using rain regime classification prior to estimation.

1. Introduction

An essential element of the satellite Tropical Rainfall Measuring Mission (TRMM) is validation of the rainfall estimates that are based on observations taken from space (Simpson et al. 1988). This will be accomplished using ground-based systems consisting of weather radars and rain gauge networks at several locations around the world. Data collected at these sites will be processed using consistent processing and estimation algorithms to produce reliable rainfall accumulation estimates at different spatiotemporal scales. The ground-based estimates will be used as a reference in evaluation of the tropical rainfall estimates based on the TRMM spacecraft observations.

This paper describes developmental efforts leading to a candidate ground-based rainfall estimation algorithm to be used as a reference in TRMM. The conversion of radar signal into a field of rainfall accumulations is a complex process consisting of many intermediate steps. The most important of them are constructing appropriate observables based on radar volume scan data, nonlinear transformation of the observables into rainfall rates, interpolation from polar to rectangular grid, constructing

Corresponding author address: Prof. Witold F. Krajewski, Iowa Institute of Hydraulic Research, University of Iowa, 404 Hydraulics Laboratory, Iowa City, IA 52242-1585.
E-mail: wkrajew@icaen.uiowa.edu

accumulations for different timescales, and overall bias adjustment. As a result, maps of rainfall intensity, as well as of hourly, daily, 5-day, and monthly accumulations are produced. The grid maps have resolution 2 km $\times$ 2 km and cover the range at 150 km centered at the radar location. Several additional procedures are included in the algorithm. These are classification of the rainfall regime into convective and stratiform types, merging of the radar and rain gauge data on the daily and higher accumulation level to minimize the estimation variance, and attenuation correction for the C-band radars.

There are several features that distinguish our approach to radar rainfall estimation from the existing procedures. One of them is a new parameterization of the *Z–R* relationship, with continuous range dependence. This study also organizes many radar rainfall estimation steps, that so far were investigated separately, into an integral data processing system. However, the most innovative feature is the methodology used to estimate the parameters that control the algorithm performance. The main algorithm contains several parameters, and their values are calibrated by minimizing a selected criterion on the final product level. This global optimization approach justifies our use of the term ''estimation'' in our methodology because a crucial element defining every legitimate statistical estimation method is optimization of some representative criterion (Bickel and Doksum 1977). Effectively, the above approach is equivalent to investigating a large number (hundreds) of *Z–R* relationships using a uniform, objective set of criteria for their evaluation. Also, this seems to be a natural way to directly control those properties of the radar rainfall final products that are most important for the users.

Observations from a C-band radar in Darwin, Australia, together with the local rain gauge network data, were used to calibrate and test our algorithm. A period of 25 days from December 1993 and January 1994 was selected for the study presented in this paper. Radar volume scans were performed every 10 min and complementary data from 54 rain gauges were available in the range of the radar rainfall map. The rain gauge measurements were split into two subsamples. The first, called a calibration sample, was used in parameter estimation and bias adjustment of the algorithm. The second, a validation sample, was used for the relatively independent validation of the algorithm performance.

The paper is organized as follows. In section 2, the structure of the algorithm and description of its components are presented. Then the algorithm parameter estimation technique is described, and some of its results are discussed. Section 4 presents briefly our implementation of a cokriging technique for merging of radar and rain gauge data. A section with discussion and conclusions completes the paper.

2. The radar rainfall estimation algorithm

a. The algorithm summary

The purpose of the estimation algorithm described here is to produce instantaneous, hourly, 1-day, 5-day, and monthly rainfall accumulation maps based on radar reflectivity volume scans and accompanying rain gauge data. The maps cover the range of 150 km from the radar site and have resolution 2 km $\times$ 2 km. The algorithm can be summarized as a sequence of the following processing steps.

1) Read the volume scan radar reflectivity (Z) information, the system parameter file, and, optionally, apply attenuation correction.
2) Construct radar reflectivity map and classify the echoes into convective and stratiform classes.
3) Integrate vertically the radar reflectivities above a specified threshold up to selected levels, which might be different for different rain regimes. Convert the integral into rainfall (R) estimates using nonlinear regression relations. The relations are different for convective and stratiform classes and include continuous distance from radar as another predictor.
4) Transform the rain rates in polar coordinates onto a Cartesian grid, with resolution 2 km $\times$ 2 km.
5) Calculate velocity vectors of the precipitation patterns using cross-correlation technique. Calculate hourly accumulation maps correcting for the advection effect.
6) Produce 1-day, 5-day, and monthly accumulation maps. Read available rain gauge data, calculate average monthly residual bias, remove the bias on each accumulation level.
7) Optionally, apply cokriging algorithm to merge radar rainfall and rain gauge accumulations for 1-day, 5-day, and monthly accumulation maps.

The algorithm can use rain gauge data with different temporal resolution. For example, it can assimilate tipping bucket (or optical) high resolution (on the order of 1 min) data, hourly data, and daily data for estimation of daily, 5-day, and monthly rainfall. The algorithm has a modular design and thus is easy to modify. This implies operational flexibility of the algorithm as it is applied to different radar sites, radar–rain gauge network configurations and the user demands.

More detailed descriptions of the most important elements of the radar rainfall estimation system are presented below.

b. Attenuation correction

The preliminary data processing step in the rainfall estimation algorithm is an attenuation adjustment for the 5-cm radar data. The adjustment was performed using an iterative procedure that is an implementation of the algorithm by Hildebrand (1978). Mathematically,

the attenuation correction along the radar beam can be formulated as a recursive system of three equations:

$$R(r) = \left[\frac{Z_a(r)}{a}\right]^{1/b} \quad (1)$$

$$K(r) = \alpha R(r)^{\beta} \quad (2)$$

$$Z_{\text{cor}}(r) = Z_a(r) + 2\sum_{x=1}^{r-1} K(x)\Delta r, \quad (3)$$

where R is the radar rainfall estimate, Z_a is the initial radar reflectivity factor, Z_{cor} is the corrected reflectivity factor, K is the specific attenuation, r is the distance from the radar, and Δr is the distance step. The specific attenuation K is defined as the attenuation of the electromagnetic wave passing through the unit distance of a medium, usually expressed in logarithmic scale (dB km^{-1}).

The values of the parameters a and b come from a power-law Z–R relationship based on a preliminary analysis of the data. They were adjusted in a traditional way by simple regression of radar reflectivities (in dBZ units) and 5-min rain gauge intensities (in dBR units). For the purpose of the attenuation correction, this simplified Z–R conversion is considered to be sufficient. The parameters α and β are from an appropriate K–R relationship, chosen based on the results by Delrieu et al. (1991). The above procedure is repeated until successive iterations do not produce significant changes in the estimated total attenuation. The results of the correction application in this study are preliminary and indicate mainly that it does not diverge. No quantitative evidence of a statistically significant improvement in the radar rainfall products has been obtained, although visual assessment of individual maps suggests that in some cases it can have a positive effect. Unfortunately, at the distances where the benefits were apparent, only very few gauges were available. Thus, this algorithm step requires further study and has been left as an optional choice for the user.

c. Rainfall regime classification

The next step, prior to rainfall estimation, is classification of the precipitation type into convective and stratiform classes based on radar reflectivity data. The microphysical properties and vertical structure of rain associated with the two precipitation regimes are often quite different (Houze 1993; Short et al. 1990). Therefore, the radar-based classification is applied prior to the rainfall estimation step.

A modified version of the method presented by Steiner et al. (1995) was used here. In summary, the technique uses the relative peakedness of the horizontal radar reflectivity patterns on a 2 km × 2 km rectangular grid and the reflectivity value as predictors of the echo type. The peakedness is defined as a difference of the reflectivity in the classified grid point and the average of the nonzero reflectivities within a radius of 11 km around the point. Then, the algorithm defines a convective zone around a point that has been classified as a convective echo. The size of the surroundings is a nonlinear function of the reflectivity at the maximum and is referred to as convective radius. Information about vertical structure of the radar echo, as well as Doppler radar data on the vertical motions, has been used for calibration and verification of this algorithm. For a detailed description of the classification technique and its validation, the reader is referred to Steiner et al. (1995).

The modification of the above technique used herein consists of application of the classification results to the radar data in polar coordinates. First, reflectivities on the map for which the algorithm by Steiner et al. (1995) was calibrated are classified into the convective and stratiform classes. Then, a polar pixel for which the center vertically projected onto a horizontal plane falls into a classified rectangular bin is attributed its class. The inverse of the coordinate transformation algorithm that will be described later is used here.

d. Conversion of radar observables into rain rates

This is the major part of the algorithm that defines most of its properties. Conversion of radar observables into rain rates is performed on the radar volume scan data in polar coordinates and consists of two operations. First, the radar reflectivities that exceed an assumed threshold are integrated in an atmospheric column up to a specified altitude. These upper levels depend on the precipitation type and are defined as parameters and easily modified. The earth's curvature and standard atmospheric refraction conditions are taken into account in determining the radar bins to be included in the vertical integration column. The following expression was applied to calculate the height of the radar beam center:

$$h = S\sin(\theta) + \frac{S^2}{2R_{\text{eff}}}, \quad (4)$$

where S is the distance of the bin from the radar, θ is the elevation angle of the radar antenna, and $R_{\text{eff}} = 8500$ km is the effective radius of the earth accounting for the standard atmospheric refraction (Doviak and Zrnić 1993). This vertical integration applies only to the regions where data from more than one radar sweep are within the upper altitude limit. Practically, it is limited to the distance 60–70 km from the radar, and, beyond this range, only the lowest scan is taken into account. The concept behind the vertical integration is to incorporate into the rainfall estimator as much relevant radar information as possible. The random error of the reflectivity measurement in a single radar bin is significant and it propagates to the rainfall estimates. Averaging of all the relevant signal available in a volume scan is an inexpensive and natural way to increase the signal-to-noise (S/N) ratio. A criterion of this relevance is the improvement of the final products.

The vertically averaged reflectivities are converted into rainfall rates on the ground using a nonlinear, power-law transformation given by the following expression:

$$R = B_0\left[\frac{Z_v}{A_x(1 + a_xS/S_o)}\right]^{[B_x(1+b_xS/S_o)]^{-1}}, \quad (5)$$

where Z_v is vertically averaged reflectivity over a horizontal polar bin; S is the distance of the bin from the radar; $S_o = 150$ km is the range of the radar rainfall estimation area; A_x, a_x, B_x, and b_x are the model parameters that depend on the precipitation regime (index x); and B_0 is an overall bias adjustment parameter. Equation (5) is a straightforward rearrangement of the traditional form of the Z–R power-law relationship, in which radar reflectivity is a function of rainfall ($Z = AR^b$), into the rainfall estimator form. Although our relationship exponent and multiplier are, in general, range dependent, for fixed distance their estimates can be compared to typical values of those parameters reported in the literature. This comparison is presented in section 3.

The above relation was chosen as the parsimonious nonlinear regression model for the rainfall estimation. The range dependence is often dealt with by constructing separate relationships for several distance ranges (e.g., Rosenfeld et al. 1994), which in some cases leads to artificial jumps of the rainfall estimates at the boundaries of the regions. In (5), the range dependence is included in the model as a continuous variable. Parameters a_x and b_x, which depend on the rain regime, control the range behavior of the multiplier and the exponent of the power-law Z–R relationship.

There is a certain degree of redundancy in the multiplication coefficients in (5). Adjusting the absolute values of the multipliers A_x, specific for the rain regimes, can be replaced by adjusting the coefficient B_0. This organization of the model parameters, however, proved to be convenient from the point of view of the implementation practice. The A_x parameters control the relative impact of different rain regimes, whereas B_0 addresses the overall estimation bias.

e. Transformation from polar to Cartesian coordinates

At this point, the radar volume data have been converted to rainfall rates at the ground in the form of a polar coordinate map that has to be transformed into a rectangular grid required both by the next processing steps and by the users of the final products. An effort to address the radar measurement geometry in the transformation algorithm was made because numerical noise introduced by inadequate spatial interpolation scheme can negatively affect the system performance. The transformation algorithm divides a radar sampling volume into 10 discrete subazimuths to pick up the spatial pattern of the radar sampling volumes. Based on this discretization, the average of the rainfall rates from the elementary subdivisions of all the radar sampling volumes that project into a Cartesian grid pixel is computed.

The implementation of the algorithm is fully parameterized to handle any combination of radar characteristics and Cartesian field specifications. The transformation from polar to Cartesian coordinates and the reverse are performed using look-up tables, which is a very fast method.

f. Rainfall accumulation and bias adjustment

The next stage in the algorithm is preparation of hourly rainfall accumulation maps. Typically, this is done by averaging all the instantaneous intensity maps that fall into a specific hourly interval. However, there is evidence (Bellon et al. 1991; Liu and Krajewski 1996) that temporal sampling effect of the radar observations combined with high advection velocity of the rainfall patterns can lead to significant errors in the spatial distribution of the radar estimated rainfall accumulations. These errors can be partially corrected using a temporal interpolation scheme that accounts for the shift of the radar field between the observations (Fabry et al. 1994). Therefore, our estimation scheme includes an advection correction procedure that converts two consecutive maps of radar rainfall intensities into accumulation over the time interval between the observations.

First, the average advection vector $\Delta\mathbf{u}_o$ is determined using the well-known cross-correlation method. The advection vector is defined as a spatial shift of the first field that maximizes the cross-correlation coefficient between the fields:

$$\rho(\Delta\mathbf{u}) = \frac{1}{\sigma_1\sigma_2}\sum_n [R_1(\mathbf{u}_n - \Delta\mathbf{u}) - \mu_1][R_2(\mathbf{u}_n) - \mu_2], \quad (6)$$

where $\Delta\mathbf{u}$ is the field shift, R_1 and R_2 are first and second radar rainfall fields, μ_i and σ_i are the average and standard deviation of the rainfall in the ith field, and the summation is over all the pixels $\mathbf{u}_n$ for which the expression under the sum is defined.

Then, the advection vector is used to calculate the time-interpolated fields every 1 min between the first and the second observation considered. The interpolated rainfall field at the time t since the first observation is calculated as a weighted average of the appropriately shifted first (forward) and second (backward) fields from

$$R_{\text{int}}(\mathbf{u}, t) = \frac{T - t}{T}R_1\left(\mathbf{u} - \frac{t}{T}\Delta\mathbf{u}_o\right) + \frac{t}{T}R_2\left(\mathbf{u} + \frac{T - t}{T}\Delta\mathbf{u}_o\right), \quad (7)$$

where T is the time difference between the first and second observation.

The field of rainfall accumulation over some time period T is then calculated from every minute rain intensities (mm h^{-1}) using the following expression:

$$R_T(\mathbf{u}) = \frac{1}{T}\sum_{t=1}^{t=T} R_{\text{int}}(\mathbf{u}, t), \quad (8)$$

which is also used to create hourly accumulation maps. The above interpolation scheme can also be effective in filling the gaps in radar observations that sometimes arise for technical reasons. The applicability of the scheme may depend on the dynamics of the precipitation system and the length of the temporal gap. The quantitative criteria for situations where advective interpolation can be applied were not investigated in this study.

The hourly rainfall maps are then used as the basis to obtain daily, 5-day, and monthly accumulation maps. These are simply calculated as sums of the hourly accumulations within the desired period. A problem that arises at this step is accounting for missing data. There were very few gaps in the dataset that were too long to fill using the advection interpolation scheme. The longest gap was 3 h. To obtain daily accumulation for a day with missing hours, those hours were substituted with the average hourly accumulation from the available hours on this day. The longer-term accumulations were then calculated from the daily results.

The last step in the basic version of our radar rainfall estimation algorithm is the adjustment of B_0, the overall bias coefficient. This is done by balancing the radar and rain gauge daily accumulations averaged over all available rain gauges and all days in the monthly period considered. Only the radar pixels that contain the rain gauge sites are taken for this comparison, and B_0 is estimated as a value for which radar and rain gauge average daily accumulations are equal. The TRMM ground validation is an off-line task in which the analysis of a monthly period is performed after all the data for this period are completed. In this setup, operational removal of the overall residual bias, based on the current data, is a part of the rainfall estimation process. Another possibility to include current rain gauge information will be discussed in section 4.

3. Parameter estimation, results, and discussion

a. Optimization methodology

Estimation of the parameters of our radar rainfall algorithm is formulated as an optimization problem based on the model described in the previous section. The optimization criterion is the minimization of the root-mean-square (rms) difference between radar based and rain gauge accumulations:

$$\text{rms} = \left\{\frac{1}{N_t N_g}\sum_{i=1}^{N_t}\sum_{j=1}^{N_g}[R_r(i,j) - R_g(i,j)]^2\right\}^{1/2}, \quad (9)$$

where R_g is the rain gauge accumulation at the jth gauge, R_r is the radar accumulation around this gauge, both for the ith time period, N_g is the number of rain gauges and N_t is the number of time periods.

TABLE 1. Estimated optimal values of the parameters of our radar rainfall estimation algorithm, together with their short descriptions. The subscripts s and c of the parameter symbols stand for stratiform and convective, respectively.

Z_0	12.0 dBZ	reflectivity threshold
$H_s = H_c$	1.5 km	upper integration boundaries
$B_s = B_c$	1.5	exponents in Eq. (5)
$b_s = b_c$	0.4	range dependence of the exponents
$A_s = A_c$	50.0	multipliers in Eq. (5)
$a_s = a_c$	0.0	range dependence of the multipliers
B_0	1.74	overall bias adjustment in Eq. (5)

This objective function is applied on the final product level to allow for integral optimization and assessment of the algorithm. The rationale behind this approach is straightforward: if good quality of the radar rainfall final products is to be obtained, why not use this quality as a criterion for the algorithm optimization. Our experience indicates that, due to the complex spatial and temporal averaging and the nonlinear transformations involved, separate optimization of selected steps, which is traditionally applied, cannot assure that the final product would also be optimal.

The choice of the accumulation period and the radar space domain associated with a gauge for this criterion is flexible and depends on the available data and the final product requirements. For the purpose of this study, the daily accumulations were used as the primary criterion. Five-day and monthly accumulation rms radar–rain gauge differences were also evaluated for control purposes. A reason for selecting the daily time interval for the primary criterion is the utilization of the daily rain gauge data for calibration and validation of the algorithm. However, physical considerations are also important. Extreme spatial variability of rainfall is a source of fundamental problems when direct comparisons of spatially averaged radar estimates and near-point rain gauge measurements are attempted (Seed and Austin 1990; Crane 1990). This is especially true for short-term accumulations. Using daily accumulations significantly reduces the effect of spatial rainfall variability on the comparison statistics.

The basic algorithm contains several parameters, most of them determined separately for convective and stratiform regimes. They are the reflectivity threshold, the lower and upper vertical averaging limits, and the coefficients of the Z–R conversion given by Eq. (5) and parameterized as linear functions of the distance from the radar. Thus, calibration of the model consists of simultaneous adjustment of 12 parameters. Their optimal values and short definitions are given in Table 1.

Due to the size of the optimization problem, employment of a global optimization algorithm, such as gradient based methods, would be prohibitively expensive. Thus, a trial-and-error procedure was applied here.

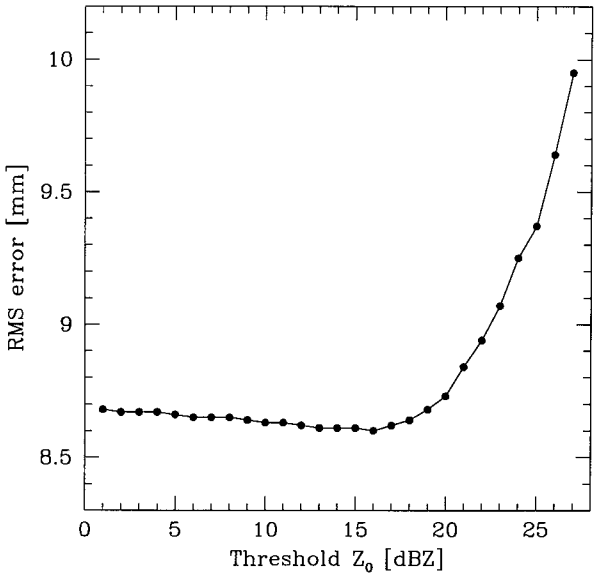

FIG. 1. The rms criterion [Eq. (9)] as a function of the reflectivity threshold Z_0. The rest of the model parameters are as in Table 1.

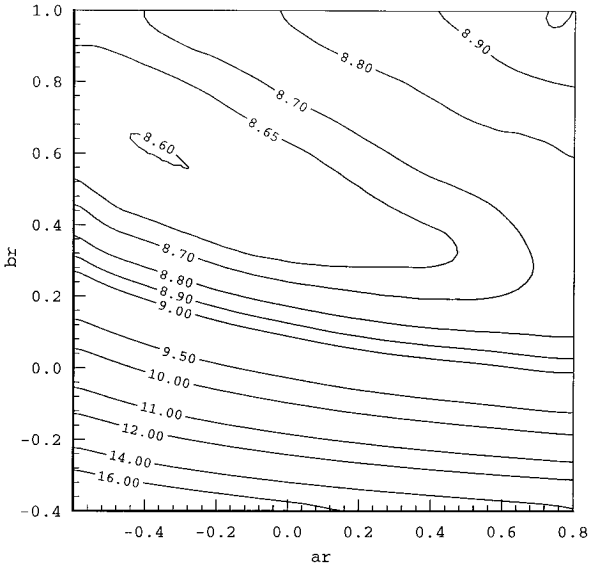

FIG. 2. The rms criterion [Eq. (9)] as a function of both range correction coefficients. The first one (*b*) is a linear correction of the exponent *B* and the second one (*a*) is a linear correction of the multiplicative coefficient of the power-law *Z–R* relationship. The rest of the model parameters are as in Table 1. The labels of the rms difference contours are in millimeters.

It is based on a large number of iterations including careful analysis of the shape of the rms objective function in several cross sections of the parameter space. As an illustration of this process and of the final results, we present in Figs. 1–7 several representative cross sections of the parameter domain containing the optimal point. The contour plots of the rms difference for chosen pairs of the parameters are especially useful to illustrate the parameter estimation process. They also show the sensitivity of the rainfall estimates to the parameter deviations.

It is important to note that the rms difference between radar estimates and rain gauge measurements cannot be interpreted as the error of the radar rainfall. The radar samples a spatial integral of the rainfall, and its domain is approximately 2 km $\times$ 2 km for the final products. The difference between this spatial average and point rain gauge sampling creates a permanent background that cannot be reduced by any improvement of the radar rainfall estimation algorithm (Ciach and Krajewski 1997). Nevertheless, if the spatial discretization of the radar products is fixed, this background is constant, and one can use the rms criterion to optimize the algorithm, to compare its different versions, and to test its sensitivity to the parameter variations.

b. Discussion of the optimization results

The first step of our processing is removing the signals that are below a certain threshold. On several occasions, weak residuals of ground clutter were observed and the purpose of the threshold was to clean the data of that noise. The effects of different threshold values on the rainfall estimates in terms of our daily rms criterion are shown in Fig. 1. The minimum is in the range of 12–16 dB*Z*. The dependence is very weak below this range, but the error increases sharply for higher thresholds. This means that all the radar signals higher than 16 dB*Z* contain information useful for rainfall estimation and applying higher threshold is unjustified. On the other hand, lower signals practically do not affect the estimation error, even if they are caused by clutter.

An important part of our model is the continuous range dependence expressed by the parameters a_x and b_x in the relation (5). These parameters proved to be practically independent of the rainfall regime but highly dependent on each other. This is demonstrated in Fig. 2 by the elongated contours of the daily rms difference versus the range dependence parameters *a* and *b* (common for convective and stratiform classes). This colinearity is evidence that the model is overdetermined and the change of one parameter over a broad range can be compensated by an appropriate adjustment of the other, without significant change of the algorithm performance. In this situation it was reasonable to remove one of the parameters to simplify the model. Figure 2 indicates that the algorithm performance is much more sensitive to changes of the *b* parameter than to variations of *a*. It also shows that removing the range dependence of the multiplier *A* by fixing $a_s = a_c = 0$ does not increase the rms criterion by more than 0.2%. Based on this evidence, the decision was made to keep only the range dependence of the exponent *B*. This also simplifies the optimization process by reducing the number of parameters to adjust.

From Fig. 2, one can obtain an estimate of the range

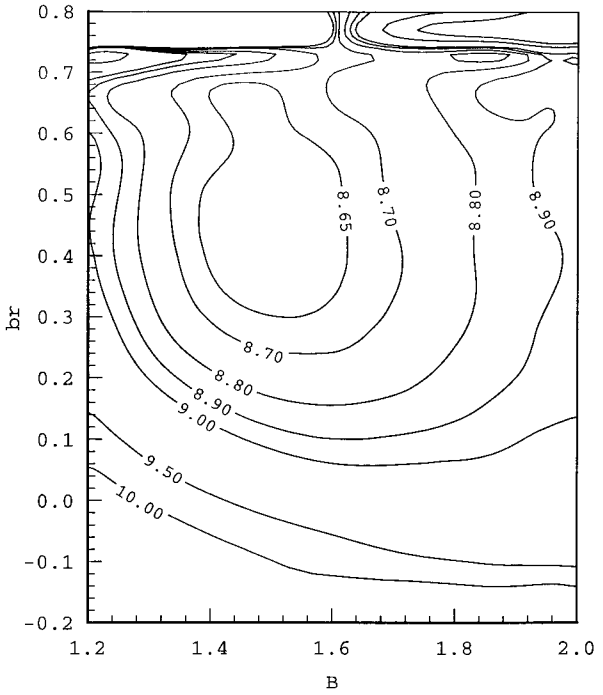

FIG. 3. The rms criterion [Eq. (9)] as a function of the exponent B of the power-law Z–R relationship and its range correction coefficient b. The rest of the model parameters are as in Table 1. The labels of the rms difference contours are in millimeters.

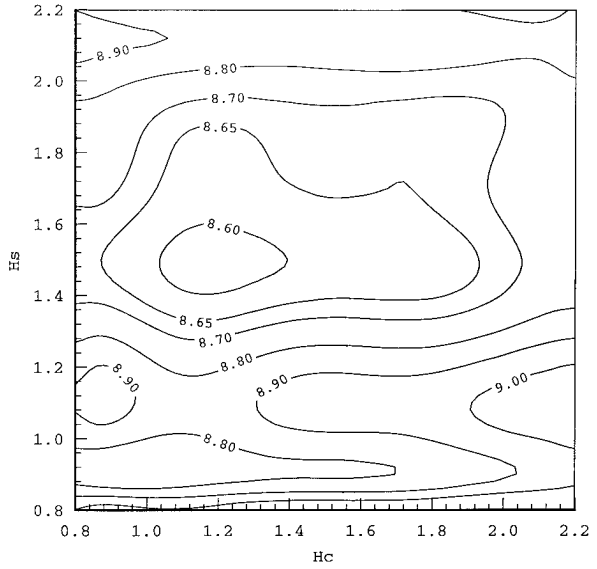

FIG. 4. The rms criterion [Eq. (9)] as a function of the upper boundaries of vertical integration for convective (H_c) and stratiform (H_s) regimes. The rest of the model parameters are as in Table 1. The labels of the rms difference contours are in millimeters.

dependence parameter b, but only for a fixed value of parameter $B = 1.5$. In general, it is reasonable to estimate the parameters b and B simultaneously because in (5) they work together as a combined range-dependent exponent. The result of this joint optimization is presented in Fig. 3. It demonstrates a well-defined minimum of the rms radar–rain gauge differences around the values of the parameters shown in Table 1. The table reports the values of $B = 1.5$ and $b = 0.4$ for the optimal exponent parameters in (5), which results in the change of the effective Z–R conversion exponent ranging from 1.5 near the radar to 2.1 at the distance of 150 km. These numbers are in the range of the Z–R exponent values reported in the literature (Battan 1973). What might be surprising, however, is the magnitude of the distance correction effect caused by the exponent change with distance. For example, radar reflectivity of 40 dBZ at the distance of 150 km will be converted to about six times lower rain rate than the same signal at close distances. This effect is opposite the effect of radar beam attenuation, which would force the algorithm to increase the impact of the distant reflectivities in order to compensate for it. However, this is a result of objective algorithm optimization, and no reports are known that would contradict it, with regard to the distance parameterization presented here. It is not obvious what the physical interpretation can be for such strong range effect. The study by Rosenfeld et al. (1992) shows qualitatively similar impacts of the reflectivity gradients on rainfall estimation if combined with large radar volume sample size. These results might suggest a possible explanation, but the effect certainly requires more experimental research.

Figure 4 shows the contour plots of the daily rms difference as a function of the upper limits of the vertical reflectivity integration for stratiform (H_s) and convective (H_c) rain regimes. The first conclusion is that there exists a well-defined minimum of the upper boundary at the level of about 1.5 km. This means that the vertical integration can increase the S/N ratio of the radar data with respect to rainfall estimation. It was also checked (not shown here) that introducing a lower boundary to reject that part of the signal that is most influenced by ground clutter does not help and in fact increases the rms criterion. This means that, for the optimization of the final product, integration from the lowest available level up to 1.5 km works better than limitation to the lowest radar sweep only, and better than any CAPPI cross section.

We are aware that operational estimation of the vertical profile of reflectivity (VPR) like, for example, in Joss and Lee (1995) would certainly work better than our simple integration, however, it was not explored in this study in which a simplified approach was assumed. On the other hand, our result suggests that in the climatic region investigated here the VPR gradients in the rain layer up to 1.5 km are generally weak. Thus, the impact of the cases with vertical gradient strong enough to negatively affect the vertical averaging of the radar signal implemented in our algorithm is insignificant from the climatological perspective.

Discussing the optimal parameter values in Table 1,

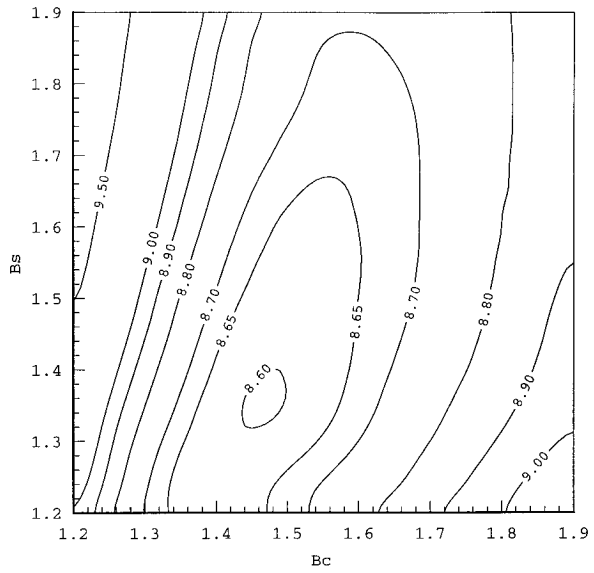

FIG. 5. The rms criterion [Eq. (9)] as a function of the exponent coefficients for convective (B_c) and stratiform (B_s) regimes. The rest of the model parameters are as in Table 1. The labels of the rms difference contours are in millimeters.

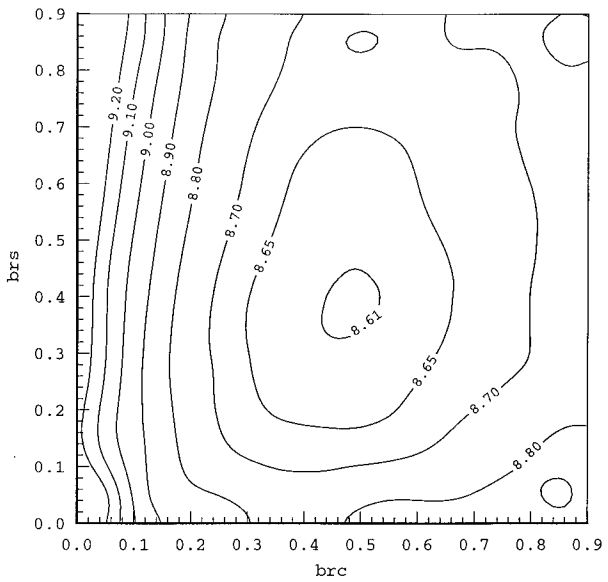

FIG. 6. The rms criterion [Eq. (9)] as a function of the exponent B range correction coefficients for convective (b_c) and stratiform (b_s) regimes. The rest of the model parameters are as in Table 1. The labels of the rms difference contours are in millimeters.

we finally want to comment on the multipliers of the Z–R conversion (5). They control the systematic bias of the radar rainfall estimation and consist of two parts. One is a set of A_x parameters associated with different rain regimes, and the other is the overall bias adjustment B_0. The Z–R relationship (5) is range dependent, but for a fixed distance it has constant coefficients and can be rearranged into the commonly quoted traditional form of $Z = AR^b$. For example, it is $Z = 21.8R^{1.5}$ near the radar, $Z = 18.4R^{1.8}$ at the 75-km distance, and $Z = 15.6R^{2.1}$ at 150 km. The values of the A parameter seem to be surprisingly low, but these are the values required to balance rain gauge and radar long-term accumulations for the data sample used in this study. We made a thorough investigation to explain the huge difference between our results and the Z–R multiplier values usually reported in the literature (between 100 and 400). To the best of our knowledge, it does not depend much on the details of the Z–R conversion and is certainly a specific feature of the radar reflectivity data used in this study. Most likely, the unusually low values of the effective A parameter originate from the particular calibration of the Darwin radar system during that period. Thanks to the operational overall bias removal, which is an inherent part of our algorithm, the final rainfall products are independent of the specific radar calibration.

c. *Effect of rain regime classification*

A large part of our analysis was devoted to testing the significance of the rain regime classification for the radar rainfall estimation. Several researchers have reported systematic differences of the rainfall microphysical properties and their influence on the Z–R relationship (Atlas and Chmela 1957; Short et al. 1990). However, it is not obvious whether there exists a simple association between these differences and the morphological properties of the observable radar patterns. The effects of the radar-based classification of the rain into convective and stratiform regimes can be analyzed in terms of the differences of the optimal algorithm parameters, which are class dependent. The question here is whether this differentiation can result in a noticeable reduction of the rms criterion (9).

Figure 4 indicates that the optimal upper boundary for the vertically integrated reflectivity is practically the same for both precipitation classes. In fact, our results suggest slightly lower integration boundary for the convective echoes. One possible explanation of this effect might be that a substantial part of rainfall accumulations in the Tropics originates from very shallow warm convective cells. It can be also noticed that the rms dependence on H_c is much weaker than on H_s (Fig. 4) and that simplification of the model by assuming a common upper integration boundary for both classes does not reduce the algorithm performance significantly.

The differences between stratiform and convective exponent parameters (B_s and B_c) and between their range dependence parameters (b_s and b_c) can be assessed from Figs. 5 and 6. Again, the conclusion is that the differences, from the point of view of rainfall estimation at daily scale, are insignificant. The lack of stratiform–convective difference in the range dependence does not agree with what one could expect based on the theoretical analysis by Rosenfeld et al. (1992). Their study suggests the crucial effect of horizontal reflectivity gra-

dients, which should be quite different for stratiform and convective precipitation systems, on the *Z–R* relationship range dependence. One possible explanation is that Rosenfeld et al. (1992) investigate the range effect on the level of radar sampling volume, whereas our algorithm treats the effect on the final product level, which is on a uniform grid. Another possibility is that classic concepts based on differentiable geometrical structures do not necessarily lead to valid results when applied to a stochastic field with complex multifractal properties. However, further investigation of the causes of this disagreement is beyond the scope of this study.

The last step concerns a simultaneous search for an optimum of the exponent ($B = B_c = B_s$, the same for convective and stratiform) and the ratio of the multipliers A_c/A_s for the convective and stratiform rainfall regimes. The use of multiple *Z–R* relationships for rainfall estimation improvement has been discussed (Joss and Waldvogel 1970; Austin 1987). The specific scenario described above was motivated by recent reports (Short et al. 1990) suggesting that when the variability of the power-law *Z–R* relationship versus types of precipitation is considered, the exponent often does not change systematically, whereas the multiplier exhibits large and systematic differences between classes. As pointed out in the previous section, the overall bias parameter B_0 takes care of the absolute values of the multipliers, so only their ratio has to be estimated by minimization of the rms difference. The result of this optimization is presented in Fig. 7. Again, the contours are elongated and exhibit a line of minima rather than one definite minimum. The existence and character of this colinearity is most likely explained by the properties of the classification algorithm, which generally associates the convective class with the highest values of reflectivity in the radar field. Thus, A_c/A_s primarily changes the relative impact of higher versus lower reflectivities in the rainfall estimate, and, while the exponent *B* in (5) works basically the same way, no additional performance improvement can be achieved from the multiplier differentiating.

Our results show that the stratiform–convective rain regime classification does not improve the performance of our radar rainfall estimation algorithm. This is in contrast with the results of Short et al. (1990), who found a strong shift between the stratiform and convective *Z–R* relationships based on analysis of point rainfall. However, our finding is in good agreement with qualitative observation by Steiner et al. (1995), which has been further confirmed by Steiner and Houze (1997) and by Yuter and Houze (1997). The conclusions of these studies should not be interpreted to mean that rainfall regime classifications are worthless for the radar rainfall estimation purposes, but rather that the dichotomic classification investigated here is not sufficient. Indirectly, our outcomes confirm the results of Rosenfeld et al. (1995), who propose much more complex classification to improve radar rainfall products.

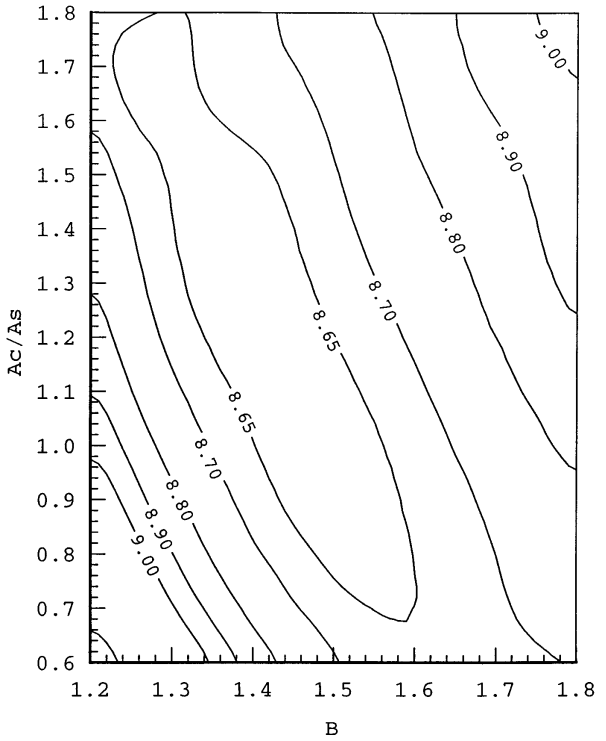

FIG. 7. The rms criterion [Eq. (9)] as a function of the exponent coefficient *B* and the ratio of the multiplicative coefficients for convective (A_c) and stratiform (A_s) regimes. The rest of the model parameters are as in Table 1. The labels of the rms difference contours are in millimeters.

d. Summary of the algorithm performance

The performance of our algorithm is summarized in Table 2. The table contains a list of both the bias error and the rms radar–rain gauge differences for daily, 5-day, and monthly (25 days) estimates. The rain gauge accumulations, also shown in the table, allow for the assessment of the relative importance of the factors. Apart from this summary statistic, the results for each day are included to demonstrate large variability of the rain conditions within the period analyzed. Note that the summary daily bias for the calibration sample is exactly zero as a result of the general bias adjustment. This does not hold for the 5-day and 25-day summaries because they are based only on such subsamples for which a full rain gauge record existed during the period. For example, the monthly summary for validation sample is based on accumulations from 13 gauges because the other gauges have gaps in their records. As a result of this sample difference, small biases of the order of 1% of the average totals occur, even for the calibration summaries. Results for both calibration and validation subsamples are presented together in Table 2 to assess stability of the algorithm. The stability is very good and, for the validation data, the bias increased to about 4% only (except for the 25-day result for which the 13 gauges are most likely not representative) and the rms

TABLE 2. Summary statistics of the radar rainfall estimation algorithm. Average gauge values, bias, and rms differences are presented for daily, 5-day, and 25-day accumulations. For the daily accumulations, the statistics for each individual day are also presented. Both calibration and validation subsamples are compared. All values are in units of millimeters.

	Calibration data			Validation data		
Date	Mean	Bias	rms	Mean	Bias	rms
24 Dec	2.12	0.64	2.42	4.42	−3.15	12.33
25 Dec	20.05	−1.70	8.02	24.52	−0.45	12.42
26 Dec	25.93	−5.92	12.77	29.68	−4.97	14.17
28 Dec	72.83	−10.28	27.18	67.87	−10.31	33.63
29 Dec	5.00	0.58	5.09	5.17	0.28	7.13
30 Dec	23.97	2.05	12.04	25.77	2.69	9.53
31 Dec	0.42	−0.11	1.84	1.39	1.04	6.23
01 Jan	6.26	0.39	5.91	5.93	0.73	5.43
02 Jan	0.00	0.01	0.07	0.00	0.00	0.00
03 Jan	0.00	0.01	0.03	0.00	0.00	0.00
04 Jan	13.27	2.62	9.42	13.85	3.10	9.48
05 Jan	0.00	0.67	2.49	0.00	0.10	0.30
06 Jan	0.59	0.91	1.84	1.38	0.65	2.52
07 Jan	25.92	−4.29	15.01	23.65	−3.18	11.19
08 Jan	3.44	2.44	4.59	2.26	1.20	3.51
09 Jan	2.34	−0.79	2.44	4.85	0.30	5.77
10 Jan	6.44	−0.26	4.85	3.19	1.59	7.96
11 Jan	13.47	2.77	8.56	11.96	3.38	9.58
12 Jan	5.94	3.52	7.01	10.52	5.43	8.98
18 Jan	3.70	2.10	4.15	6.93	1.82	5.48
19 Jan	4.77	1.30	4.11	5.85	0.95	3.85
20 Jan	1.41	0.72	2.27	0.63	1.30	2.67
21 Jan	9.31	4.88	10.84	5.62	4.61	6.71
22 Jan	1.78	−0.63	4.92	1.62	−0.26	1.45
23 Jan	5.23	0.51	3.49	5.26	0.31	4.08
ALL	10.44	0.00	8.62	9.92	0.43	9.39
5-day accumulations:						
	52.86	−0.38	20.69	50.53	2.28	25.88
25 day accumulations:						
	254.71	−3.33	42.94	257.67	28.48	54.08

differences did not increase dramatically. This optimistic assessment might be influenced by the fact that the validation gauges are placed in the vicinity of the calibration gauges, and thus are not fully independent. However, designing and carrying out a full cross-validation experiment with various scenarios of the data sample split is a nontrivial and time-consuming task (Efron and Gong 1983; Efron and Tibshirani 1993) that is beyond the scope of this paper. The relative rms criterion, defined as the rms radar–rain gauge difference divided by the corresponding average total, depends on the accumulation time. It is about 100% for daily, about 50% for 5-day, and about 20% for monthly accumulations, based on the validation sample. A major part of this effect is associated with the increased smoothness of the rainfall field with the accumulation time, which implies better representativeness of the rain gauge for the 2 km × 2 km radar rainfall area.

4. Cokriging adjustment procedure

An optional element of our radar rainfall estimation system is a spatial adjustment of daily, 5-day, and monthly accumulation maps to the corresponding rain gauge data. This presents an opportunity for using optimal interpolation techniques such as those described by Krajewski (1987), Seo et al. (1990a), Seo et al. (1990b)), or Seo and Smith (1991). Feasibility of such an adjustment depends on the rainfall accumulation variability in space at a given temporal scale and on the density and configuration of the rain gauge network.

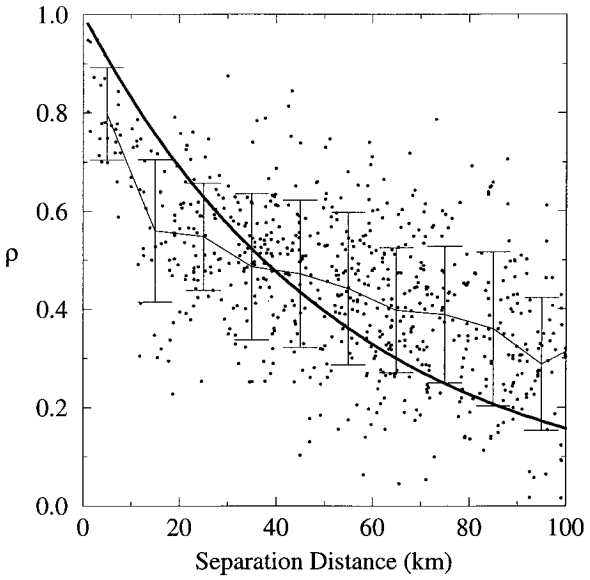

FIG. 8. Daily rainfall spatial correlation function in Darwin. The points represent correlation coefficients for pairs of rain gauges. The heavy continuous curve is the least squares fit of the exponential function. The correlation distance estimated from this fit is 55 km. The light continuous curve joins average values of the correlation coefficients for all points within 10-km distance increments. The light vertical lines indicate one-sigma confidence intervals for each average.

In this work, cokriging was used for the optimal merging of radar and rain gauge rainfall accumulations at the daily scale. The cokriging equation used in our system is

$$\hat{V}(\mathbf{u}_o) = \sum_{i=1}^{N_G} \lambda_{G_i} G_i(\mathbf{u}_i) + \sum_{i=1}^{N_R} \lambda_{R_i} R_i(\mathbf{u}_i), \qquad (10)$$

where $\hat{V}(\mathbf{u}_o)$ is the estimate of the mean area precipitation over grid square $\mathbf{u}_o$, $G_i(\mathbf{u}_i)$ are the rain gauge rainfall values, $R_i(\mathbf{u}_i)$ are the radar rainfall values, and λ_{G_i} and λ_{R_i} are the corresponding coefficients (weights) that are estimated by solving of the cokriging system, as described by Krajewski (1987). The number of 2 km × 2 km radar pixels around $\mathbf{u}_o$ that are taken into account is N_R and the number of rain gauge observations is N_G. In our application, $N_R = 5$ and the effective N_G is determined for each location by the spatial rainfall correlation function, which is based on the climatological data. Figure 8 shows the daily rainfall correlation function based on long-term rain gauge records. Each point is based on a minimum of 30 data pairs. The plot

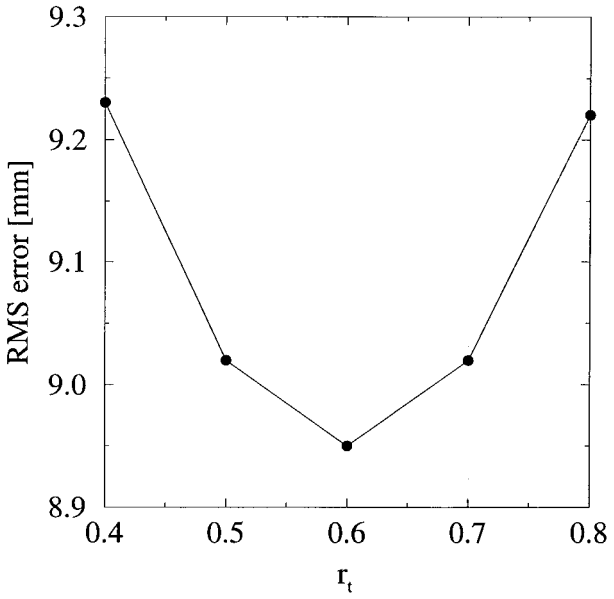

FIG. 9. Calibration curve of one of the cokriging procedure parameters. The rms difference is calculated using the cross-validation technique described in the text. The parameter r_t is the correlation between the radar rainfall estimate and the true area rainfall.

indicates that the correlation distance, defined in terms of exponential decay (e^{-1}), is about 55 km.

For optimal performance, the cokriging parameters r_t and g_t have to be determined, where r_t is the correlation between the radar estimate and the true mean area precipitation over the radar grids, whereas g_t is the correlation between the rain gauge and the true mean area precipitation over the grid squares containing the gauges. These coefficients can be interpreted in terms of the measurement precision of rain gauge and radar sensors (Krajewski 1987). Calibration was performed to determine the optimal values of r_t and g_t, after all the other parameters of our algorithm had been fixed in the way described in the previous section. The performance criterion for this optimization was the same rms radar–rain gauge difference (9). The calibration was performed using a cross-validation approach based on the calibration sample only. Each gauge value was compared with the field value at the rain gauge location estimated by cokriging of the radar rainfall with other rain gauges. Figure 9 shows results from this cross-validation tuning. The minimum rms was obtained using $r_t = 0.6$ and $g_t = 0.9$, although for this value of r_t, the rms was not sensitive to different values of g_t.

Table 3 compares results obtained with and without cokriging using the validation sample only. There is a significant quantitative improvement in all error statistics after cokriging. For example, daily rms difference for the validation locations drops from about 9.6 mm to about 7.5 mm, after its application. This rms criterion reduction is much bigger than what could be obtained using the basic estimation model (5). These results show

TABLE 3. Comparison of the error statistics of radar rainfall accumulations estimated without and with cokriging adjustment. Results are based only on validation sample. Both rms and bias error statistics are presented for daily, 5-day, and monthly accumulation periods.

	rms (mm)	Bias (mm)
1-day		
No cokriging	9.39	0.43
With cokriging	7.53	0.12
5-day		
No cokriging	25.88	2.28
With cokriging	18.54	0.97
25-day		
No cokriging	54.08	28.48
With cokriging	20.57	10.31

that the cokriging technique is a promising statistical tool to improve the radar rainfall estimates.

A part of the rainfall estimation improvement demonstrated in Table 3 might be attributed to the proximity of the validation gauges to the gauges used in estimating the daily fields. This unfortunate choice of the validation sample brings up an interesting problem. What should be a configuration of calibration/validation network for a meaningful evaluation of the performance of cokriging? If the validation network is located far away from the calibration network, the technique, by construction based on spatial correlation function, will not show any benefit. On the other hand, if the two networks are too close to each other, it casts a shadow of doubt on the real benefit, giving a perception of an artificial fit. The best approach seems to be full cross-validation through subsequent withholding of all the individual gauges, combined with modern estimation error analysis (Efron and Tibshirani 1993).

5. Summary and concluding remarks

A multicomponent radar rainfall estimation algorithm and a method of its parameter estimation are presented. Their practical implementation provide statistically and physically based tools for ground validation of the space-based rainfall estimates. They also create an excellent base for systematic studies of climatological and operational radar rainfall estimation schemes and for their intercomparison. Several features make our approach distinct from other algorithms known from the literature. It cannot be represented simply in terms of applying an arbitrary Z–R relationship. The procedure is formulated in terms of a multiparameter statistical model where distance from radar is treated as one of the continuous estimation predictors. This can be easily extended to include more rainfall predictors.

The model is optimized by using an objective function (9) on the level of the final radar rainfall products. For the purpose of this study, the rms radar–rain gauge difference of the daily accumulations was selected as an optimization criterion. This global optimization ap-

proach enables interpretation of the results in terms of statistical estimation theory. It also allows for an assessment of the relative importance of various parts of the algorithm in the full context of the rainfall estimation. This assessment was only partially explored in this paper as our goal was to present the algorithm and its main features first.

The general conclusion from the contour plots of the rms radar–rain gauge differences presented in section 3 is that our model is fairly insensitive to the parameter change around the optimal point. The rms minimum in the parameter space exists, but its vicinity is rather flat. This means that the potential for the improvement of the radar rainfall estimation based on direct reflectivity transformation (Z–R relationships) is limited. Probably, based on radar reflectivity only, further reduction of the radar estimate error variance cannot be very successful. One attempt at utilizing additional radar-derived information was to apply rainfall regime classification based on radar pattern morphology. Our analysis suggests that no significant improvement can be achieved from this. From the point of view of radar rainfall estimation, the classification used here seems to be equivalent to separation of weaker and stronger echoes only. Another conclusion is that the radar-based rainfall regime classification, and the one considered by Short et al. (1990), which is based on the features of the rainfall drop size distribution, are apparently not as close as is sometimes expected. This direction, although by no means unimportant, is not explored here.

To reduce the temporal sampling error, an interpolation scheme that accounts for the advection effects was applied. Verification of the scheme performance was done by comparison of the estimation error statistics in Table 2 with the same statistics calculated without the advection interpolation. No significant improvement was detected this way. It is very likely that, on the daily and longer scales, the temporal radar sampling error is negligible since the sampling time interval of 10 min is relatively very short. On the other hand, visual effects of the discrete temporal sampling, which were more pronounced for shorter accumulation periods, were observed in some cases. The investigation of the advection correction scheme is continuing to get more insight into its performance at different timescales.

Finally, an important result of the optimization of our algorithm is the simplification of the model. The two sets of parameters for the stratiform and convective classes was reduced to one set. To grasp the effects of the distance from the radar, one parameter describing a linear dependence of the exponent B in (5) proved to be sufficient. As a result, the final algorithm is easier to calibrate and more stable when applied to independent data.

Acknowledgments. This work was supported by NASA Grant NAG 5-2084. G. J. Ciach was supported by the NASA Graduate Student Fellowship in Global Change Research, NASA reference 4146-GC93-0225 (Award NGT 30160), and by the United States Agency for International Development under Grant HRN-5600-G-00-2037-00. J. R. McCollum was supported by the NASA Graduate Student Fellowship in Global Change Research, NASA Reference 4018-GC93-0098 (award NGT 30192). The authors appreciate this support. The authors gratefully acknowledge insightful discussions and helpful support by Robert Houze and by all organizers and participants of the Algorithm Intercomparison Workshops (AIW) that were part of the NASA TRMM Ground Validation Project. The TRMM Office prepared good quality data used in this study. Insightful remarks on this manuscript by Matthias Steiner from the Department of Civil Engineering and Operations Research of Princeton University and discussions with V. Chandrasekar from the Electrical Engineering Department of Colorado State University are also gratefully acknowledged. Finally, we want to thank an anonymous reviewer for her/his thoughtful comments and stimulating remarks.

REFERENCES

Atlas, D., and A. C. Chmela, 1957: Physical-synoptic variations of drop-size parameters. Preprints, *Sixth Weather Radar Conf.*, Cambridge, MA, Amer. Meteor. Soc., 21–29.

Austin, P. M., 1987: Relation between measured radar reflectivity and surface rainfall. *Mon. Wea. Rev.*, **115,** 1053–1070.

Battan, L. J., 1973: *Radar Observation of the Atmosphere.* The University of Chicago Press, 324 pp.

Bellon, A., F. Fabry, and G. L. Austin, 1991: Errors due to space–time sampling strategies in high resolution radar data used in hydrology. Preprints, *25th Conf. on Radar Meteorology*, Paris, France, Amer. Meteor. Soc., 2040–2048.

Bickel, P. J., and K. A. Doksum, 1977: *Mathematical Statistics: Basic Ideas and Selected Topics.* Holden-Day, 492 pp.

Ciach, G. J., and W. F. Krajewski, 1997: Error separation in remote sensing rainfall estimation. Preprints, *13th Conf. on Hydrology*, Long Beach, CA, Amer. Meteor. Soc., 137–140.

Crane, R. K., 1990: Space–time structure of rain rate field. *J. Geophys. Res.*, **95,** 2011–2020.

Delrieu, G., J. D. Creutin, and I. Saint-Andre, 1991: Mean K–R relationships: Practical results for typical weather radar wavelengths. *J. Atmos. Oceanic Technol.*, **8,** 467–476.

Doviak, R. J., and D. S. Zrnić, 1993: *Doppler Radar and Weather Observations.* Academic Press, 562 pp.

Efron, B., and G. Gong, 1983: A leisurely look at the bootstrap, the jackknife, and cross-validation. *Amer. Stat.*, **37,** 36–48.

——, and R. Tibshirani, 1993: *An Introduction to the Bootstrap.* Chapman & Hall, 436 pp.

Fabry, F., A. Bellon, M. R. Duncan, and G. L. Austin, 1994: High resolution rainfall measurements by radar for very small basins: The sampling problem reexamined. *J. Hydrol.*, **161,** 415–428.

Hildebrand, P. H., 1978: Iterative correction for attenuation of 5 cm radar in rain. *J. Appl. Meteor.*, **17,** 508–513.

Houze, R. A., Jr., 1993: *Cloud Dynamics.* Academic Press, 573 pp.

Joss, J., and A. Waldvogel, 1970: A method to improve the accuracy of radar-measured amounts of precipitation. Preprints, *14th Radar Meteorology Conf.*, Tucson, AZ, Amer. Meteor. Soc., 237–238.

——, and R. Lee, 1995: The application of radar–gauge comparisons to operational precipitation profile correction. *J. Appl. Meteor.*, **34,** 2612–2630.

Krajewski, W. F., 1987: Co-kriging of radar-rainfall and rain gage data. *J. Geophys. Res.,* **92,** 9571–9580.

Liu, C., and W. F. Krajewski, 1996: A comparison of methods for calculation of radar-rainfall hourly accumulations. *Water Resour. Bull.,* **32,** 305–315.

Rosenfeld, D., D. Atlas, D. B. Wolff, and E. Amitai, 1992: Beamwidth effects on *Z–R* relations and area-integrated rainfall. *J. Appl. Meteor.,* **31,** 454–464.

——, D. B. Wolff, and E. Amitai, 1994: The window probability matching method for rainfall measurement with radar. *J. Appl. Meteor.,* **33,** 682–693.

——, E. Amitai, and D. B. Wolff, 1995: Improved accuracy of radar WPMM estimated rainfall upon application of objective classification criteria. *J. Appl. Meteor.,* **34,** 212–223.

Seed, A., and G. L. Austin, 1990: Variability of summer Florida rainfall and its significance for the estimation of rainfall by gauges, radar and satellite. *J. Geophys. Res.,* **95,** 2207–2215.

Seo, D.-J., and J. A. Smith, 1991: Rainfall estimation using raingages and radar: A bayesian approach. *J. Stoch. Hydrol. Hydraul.,* **5,** 1–14.

——, W. F. Krajewski, and D. S. Bowles, 1990a: Stochastic interpolation methods used for multiple sensor rainfall estimation, experimental design, 1. *Water Resour. Res.,* **26,** 469–478.

——, ——, ——, and A. Azimi-Zonooz, 1990b: Stochastic interpolation methods used for multiple sensor rainfall estimation, results, 2. *Water Resour. Res.,* **26,** 915–924.

Short, D., T. Kozu, and K. Nakamura, 1990: Rainfall and raindrop size distribution observations in Darwin Australia. *Proc. URSI-F Open Symp. on Regional Factors in Predicting Radiowave Attenuation Due to Rain,* Rio de Janeiro, Brazil, Union of Radio Science International, 35–40.

Simpson, J., R. F. Adler, and G. R. North, 1988: A proposed Tropical Rainfall Measuring Mission (TRMM) satellite. *Bull. Amer. Meteor. Soc.,* **69,** 278–295.

Steiner, M., and R. A. Houze Jr., 1997: Sensitivity of the estimated monthly convective rain fraction to the choice of *Z–R* relation. *J. Appl. Meteor.,* **36,** 452–462.

——, ——, and S. E. Yuter, 1995: Climatological characterization of three-dimensional storm structure from operational radar and rain gauge data. *J. Appl. Meteor.,* **34,** 1978–2007.

Yuter, S. E., and R. A. Houze Jr., 1997: Measurements of raindrop size distributions over the Pacific warm pool and implications for *Z–R* relations. *J. Appl. Meteor.,* in press.